Structural Studies of MCM-48 Derivatized with (1,1′-Ferrocenediyl)dimethylsilane

Paula Ferreira,[a] Isabel S. Gonçalves,[a] Fred Mosselmans,[b] Martyn Pillinger,[a] João Rocha,*[a] and Alan Thursfield[a]

Keywords: Mesoporous materials / MCM-48 / Immobilization / (1,1′-Ferrocenediyl)dimethylsilane / ^{13}C and ^{29}Si solid-state NMR / Sandwich-complexes

The walls of the cubic mesoporous silicate MCM-48 have been grafted with ferrocenyl end groups by a ring-opening reaction of the *ansa*-bridged ferrocene [Fe{(η-C_5H_4)$_2$SiMe$_2$}], carried out in a pentane solution at room temperature. The orange product has been characterized by elemental analysis, powder X-ray diffraction, ^{13}C and ^{29}Si solid-state NMR, N_2 adsorption measurements, and Fe K-edge EXAFS. A high loading has been obtained (8.18 mass % Fe) and, as a result of the inclusion of the organometallic moiety, the N_2 adsorption isotherm exhibits a lower uptake. Direct structural evidence for the surface attachment of both single ferrocenyl and short chain oligo(ferrocenyl) fragments has been obtained.

Introduction

Interest in the inclusion chemistry of mesoporous oxides has accelerated since the report in 1992 by researchers at the Mobil Corporation of the discovery of a new generation of liquid crystal surfactant templated aluminosilicates,[1] distinguished by having highly ordered structures with high surface areas (1000 m^2 g^{-1}), high pore volumes (1 cm^3 g^{-1}), and very narrow pore-size distributions, tuneable in the range 20−100 Å. The so-called M41S family includes the thermally stable hexagonal MCM-41 and cubic MCM-48 phases. Their unique properties have stimulated research in areas that include sorption and phase transitions in confined spaces, ion exchange, the formation of intrachannel metal, metal oxide, and semiconductor clusters, and inclusion of metal complexes and other guests.[2] Like the commonly used silica and alumina supports, the inner surfaces of these mesoporous hosts contain pendant Si−OH groups (silanols) that enable covalent anchoring of functional groups to the channel walls. Potential applications include heterogeneous catalysis and photocatalysis involving bulky grafted catalysts and/or the conversion of large substrates, separation, removal of heavy metals, and chromatography. Our objective is the immobilization of relevant complexes on the surfaces of these mesoporous supports.

Much of the published work to date has been centred on MCM-41 as the mesoporous host. In contrast, little has been reported regarding MCM-48 which has a very different lattice. The pore system in MCM-41 is simple and consists of a hexagonal arrangement of parallel one-dimensional channels. MCM-48 possesses a complex pore architecture consisting of two mutually intertwined but unconnected three-dimensional nets. It is assumed that the silica interface resembles a minimal surface of the gyroid type.[3] Recently, O′Brien et al. showed that the walls of MCM-41 may be functionalized with ferrocenyl end groups by a ring-opening reaction with the strained metallocenophane [Fe{(η-C_5H_4)$_2$SiMe$_2$}].[4] We have followed up this work and now wish to report structural studies on MCM-48 functionalized with (1,1′-ferrocenediyl)dimethylsilane. The results are compared with MCM-41. All materials have been fully characterized by elemental analysis, powder X-ray diffraction, N_2 adsorption, magic-angle spinning (MAS) NMR (^{13}C, ^{29}Si) and Fe K-edge EXAFS spectroscopies.

Results and Discussion

Synthesis and Spectroscopic Characterization

The synthesis and some reaction chemistry of (1,1′-ferrocenediyl)dimethylsilane and other derivatives have been reported, and it was found that [1]ferrocenophanes are susceptible to nucleophilic attack by ROH.[5] This ring-opening reaction is responsible for the persistent attachment of the [Fe{(η-C_5H_4)$_2$SiMe$_2$}] unit to surfaces. Like silica and alumina supports, MCM-48 should be capable of surface reactions via terminal silanol groups.

Mixing of a suspension of MCM-48 with excess of the organometallic (1,1-ferrocenediyl)dimethylsilane in pentane at room temperature for 24 hours gives an orange solid MCM-48/[Fe{(η-C_5H_4)$_2$SiMe$_2$}] (**1**, Scheme 1). The air-stable powder was washed with pentane to remove a small portion of converted ferrocene and some unchanged [Fe{(η-C_5H_4)$_2$SiMe$_2$}].

Elemental analysis indicated that a high loading of [Fe{(η-C_5H_4)$_2$SiMe$_2$}] in the material had been achieved (8.18% mass Fe). The powder X-ray diffraction pattern of

---

[a] Department of Chemistry, University of Aveiro,
3810-193 Aveiro, Portugal
Fax: (internat.) + 351-34/370-084
E-mail: ROCHA@DQ.UA.PT
[b] CLRC Daresbury Laboratory,
Warrington, Cheshire, WA4 4AD, UK

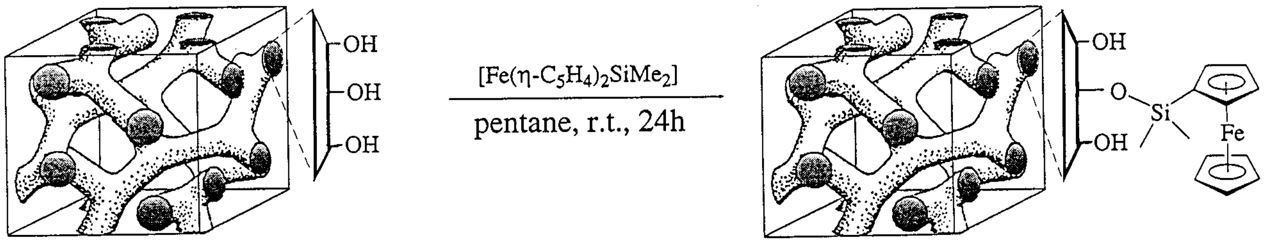

MCM-48

MCM-48

Scheme 1. Functionalization of MEM-48 with $[Fe(\eta\text{-}C_5H_4)_2SiMe_2]$

parent MCM-48 (Figure 1) can be indexed on a cubic unit cell (using the strongest reflection, d_{211}, $a = 88.616$ Å). The pattern of functionalized MCM-48 is consistent with retention of the cubic mesoporous structure. The strongest peak shifts slightly ($a = 86.559$ Å). In addition, the observed slight decrease in peak intensities does not necessarily reflect a decrease in the order of the structure but could instead be due to a decrease in the scattering contrast between the silica framework and the pores as a result of inclusion of the ferrocenyl groups.[6]

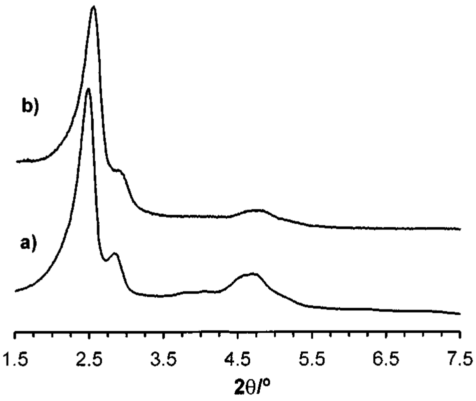

Figure 1. Powder X-ray diffraction patterns of a) as-synthesized and b) functionalized MCM-48

Solid-State NMR Studies

The ^{29}Si-CP MAS NMR spectrum of functionalized MCM-48 (Figure 2) exhibits two broad overlapping peaks $\delta = -108.8$ and -101.5, assigned to the Q_4 and Q_3 units of the silica framework, respectively. A small amount of Q_2 environments (faint peak at $\delta = -91.2$) is also present $[Q_n = Si(OSi)_n(OH)_{4-n}]$. Both the ^{29}Si CP MAS and MAS NMR spectra clearly show that upon functionalization the intensity of the Q_3 (and Q_2) peak decreases considerably. This result is consistent with the observed large decrease in the intensity of the IR absorption-band associated with OH groups on the silica surface [ν(OH) = 3742 cm^{-1}].[7] Functionalized MCM-48 also displays two strong resonances at high-frequency. The peak at $\delta = 6.5$ may be assigned to Si−O−**Si**Me$_2$Fc environments (Fc = ferrocenyl group),[4] and the signal at $\delta = -6.4$ has been previously assigned to the bridging silicon atoms in small oligomeric units of poly(ferrocenylsilane), the first unit of which is bound to the channel wall.[8] A third faint peak is seen at $\delta = -2.3$. At present, we are unable to assign this resonance.

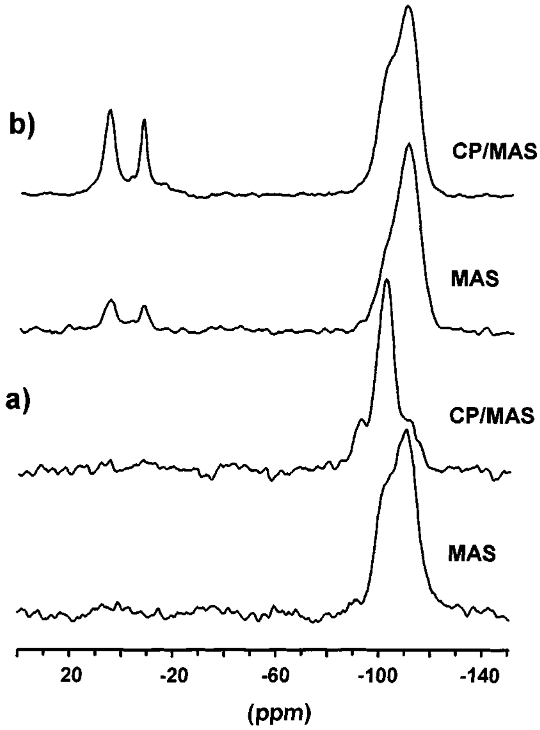

Figure 2. ^{29}Si-CP MAS and MAS NMR spectra of a) as-synthesized and b) functionalized MCM-48

The solid-state ^{13}C-CP MAS NMR spectrum of MCM-48/$[Fe\{(\eta\text{-}C_5H_4)_2SiMe_2\}]$ (**1**) is shown in Figure 3. The spectrum exhibits three resonances at $\delta = 72.3$, 68.6 and 0.1, attributed to C_5H_4Si, C_5H_5, and $SiMe_2$, respectively. The unusually high-field resonance at $\delta = 33.5$, for the cyclopentadienyl carbon attached to silicon in the $[Fe\{(\eta\text{-}C_5H_4)_2SiMe_2\}]$, shifted to a more conventional value $\delta = 72.3$ in the spectrum of the material **1**.

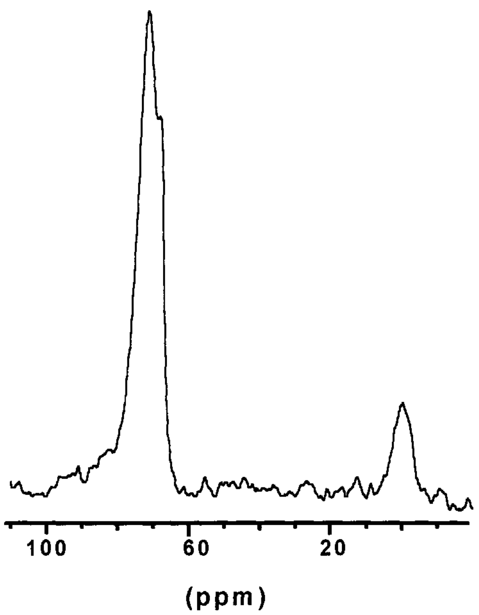

Figure 3. ^{13}C CP MAS spectrum of functionalized MCM-48

N_2 Adsorption Studies

The calcined MCM-48 sample gave a type IV N_2 adsorption isotherm (Figure 4) as designated in the IUPAC classification,[9] which is typical of a mesoporous solid and is comparable to that reported by other workers for cubic mesoporous MCM-48.[10] A well-defined step, and sharp inflection between relative pressure P/P_o = 0.3 and 0.4 corresponds to capillary condensation and suggests a rather narrow pore size distribution. The calcined MCM-41 sample also gave a type IV N_2 adsorption isotherm.

BET surface areas were calculated with the average area occupied by a N_2 molecule in the monolayer taken as 16.2 Å^2. Values of 770 m^2 g^{-1} and 970 m^2 g^{-1} were obtained for MCM-48 and MCM-41, respectively. The N_2 adsorption isotherms of the functionalized MCMs are quite different from those of the parent materials, demonstrating a lower uptake. Diffusion of N_2 through the pore system of the functionalized MCM-41 material was found to be extremely slow, hence the isotherm presented is produced from nonequilibrium points, but it serves to indicate the greatly reduced uptake. These results indicate that the free pore volume of the materials has been reduced as a result of immobilization of ferrocenyl fragments on the internal surface of the mesoporous hosts. In support of this conclusion, the BET surface areas decreased to 500 m^2 g^{-1} for MCM-48 and 270 m^2 g^{-1} for MCM-41, although of course the latter value is based on nonequilibrium data but again serves as a general indicator.

EXAFS Studies

The Fe K-edge EXAFS of MCM-41 and MCM-48 derivatized with [Fe{(η-$C_5H_4)_2SiMe_2$}] were analysed by beginning with a model of ferrocene for the Fe centre, and therefore selecting a single shell of ten carbon atoms (fit A). Refinement gave very similar theoretical fits to both EXAFS spectra and very similar structural parameters with an average Fe−C bond length of 2.06−2.07 Å and a Debye-Waller factor of 0.011−0.012 Å^2 (Table 1).

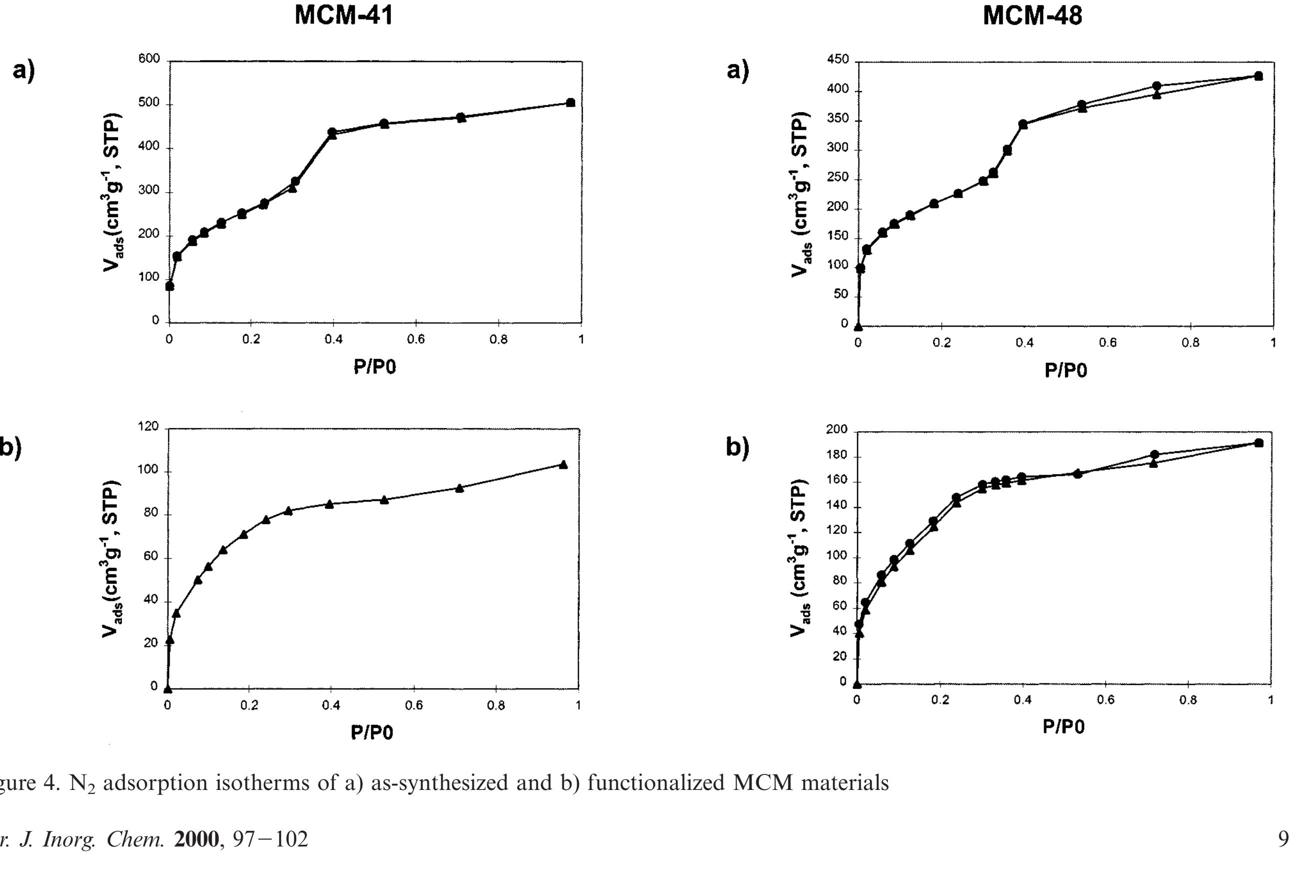

Figure 4. N_2 adsorption isotherms of a) as-synthesized and b) functionalized MCM materials

Table 1. The Fe K-edge EXAFS-derived structural parameters for [Fe{(η-C_5H_4)$_2$SiMe$_2$}], MCM-41/[Fe{(η-C_5H_4)$_2$SiMe$_2$}] and MCM-48/[Fe{(η-C_5H_4)$_2$SiMe$_2$}]

	fit	T[a]	N[b]	r[c]/Å	$2\sigma^2$[d]/Å^2	$E°$/eV	R (%)[e]
[Fe{(η-C_5H_4)$_2$SiMe$_2$}]	A	C	10	2.019(7)	0.0242(20)	−1.2	52.7
	B	C	4.3(3)	2.053(3)	0.0069(12)	−9.1	27.6
MCM-41/[Fe{(η-C_5H_4)$_2$SiMe$_2$}]	A	C	10	2.064(3)	0.0115(9)	−8.7	31.3
	B	C	8.5(7)	2.068(3)	0.0089(8)	−9.7	30.1
MCM-48 /[Fe{(η-C_5H_4)$_2$SiMe$_2$}]	A	C	10	2.070(4)	0.0109(9)	−9.7	29.0
	B	C	8.5(7)	2.075(3)	0.0084(8)	−10.9	26.9

[a] T = Atom type. – [b] N = Coordination number. Note that the errors in EXAFS-derived coordination numbers for well-defined shells are generally accepted to be of the order 20%. – [c] r = interatomic distance (standard deviations in parentheses). The systematic errors in bond lengths arising from data collection and analysis procedures are ± 0.02–0.03 Å for well-defined coordination shells. – [d] Debye–Waller factor; σ = root-mean-square deviation of interatomic distance about r. – [e] R factor = $(\Sigma|\chi^{calc} - \chi^{exp}|\, k^3 dk / \Sigma|\chi^{exp}|\, k^3 dk) \times 100\%$.

These results are comparable to those reported by O'Brien et al. for MCM-41 modified with the same complex (10 carbons at 2.045 Å, $2\sigma^2$ = 0.007 Å^2).[4] The coordination number for this shell was subsequently refined, and in both cases the best fits were obtained with a value of about 8.5 (fit B, Figure 5). It may be concluded therefore that the structural integrity of the ferrocenyl units has remained intact in the functionalid MCMs, given that errors in EXAFS-derived coordination numbers for well defined shells are generally accepted to be of the order of 20%. Additional shells in the model for nonbonded silicon or carbon atoms were not reliable as either the resulting structural parameters were poorly defined (high statistical errors) or the decrease in the fit index was not statistically significant.

In the fit to the Fe K-edge EXAFS of (1,1-ferrocenediyl)-dimethylsilane (fit A, 10 carbon atoms), the refined Fe–C bond length was slightly shorter (2.02 Å) and the Debye–Waller factor was significantly higher (0.024 Å^2) than the corresponding values obtained for the derivatized MCMs (Table 1). Overall the fit was much poorer (R-factor 52.7%). The high Debye–Waller factor is indicative of high thermal and/or static disorder in the Fe–C bond. In this *ansa*-bridged ferrocene, the cyclopentadienyl rings are tilted with respect to one another by an angle of 20.8°, the compound is appreciably strained and there is significant departure from planarity at the *ipso* carbon atom.[12] These factors are responsible for the compounds reactivity to ring-opening polymerizations. The iron lies closer to the *ipso* carbon and the two carbons adjacent to it than the two opposite it. The resulting wide and nonsymmetric distribution in Fe–C bond lengths (1.99–2.07 Å) explains the high EXAFS-derived Debye–Waller factor and the inadequate fit to the EXAFS. Attempts to fit more than one shell for bonded carbon atoms were unsuccessful. In contrast the shell of ten carbon atoms in fit A for the MCM-supported materials was well-defined and this is good evidence that the ring strain in the organometallic guest molecule has been released, i.e., that a ring-opening reaction has occurred and the cyclopentadienyl ligands are parallel, resulting in a narrower and more symmetric distribution in Fe–C bond lengths.

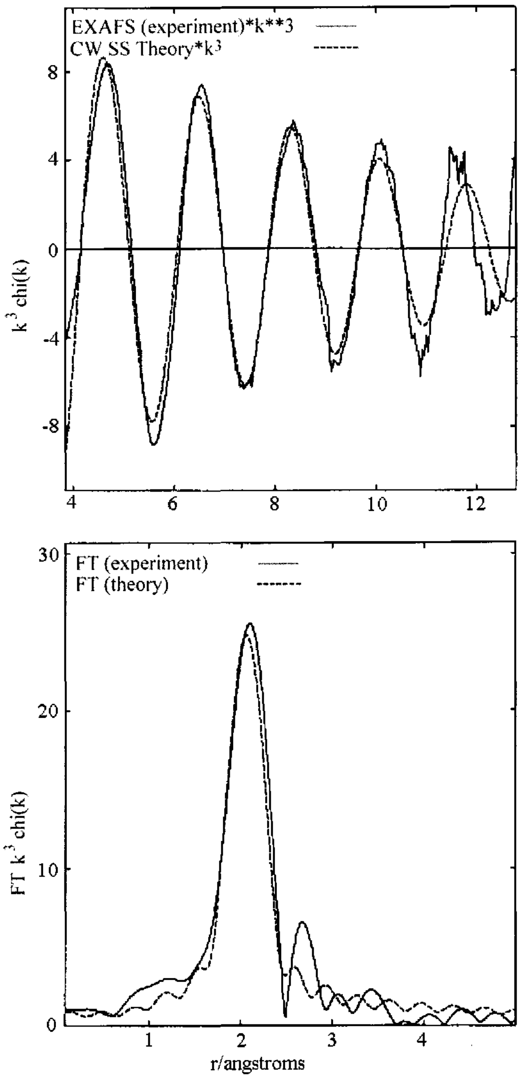

Figure 5. Fe K-edge k^3-weighted EXAFS spectrum and Fourier transform, phase-shift corrected for carbon (—— experimental; ------- curved wave theory, fit B in Table 1) of functionalized MCM-48 at 298 K.

An attempt was made to improve the model for [Fe{(η-C_5H_4)$_2$SiMe$_2$}] by including a shell for nonbonded silicon, expected at 2.69 Å. This resulted in a modest improvement in the fit and a reasonable value for the distance but the statistical errors for the structural parameters of this shell

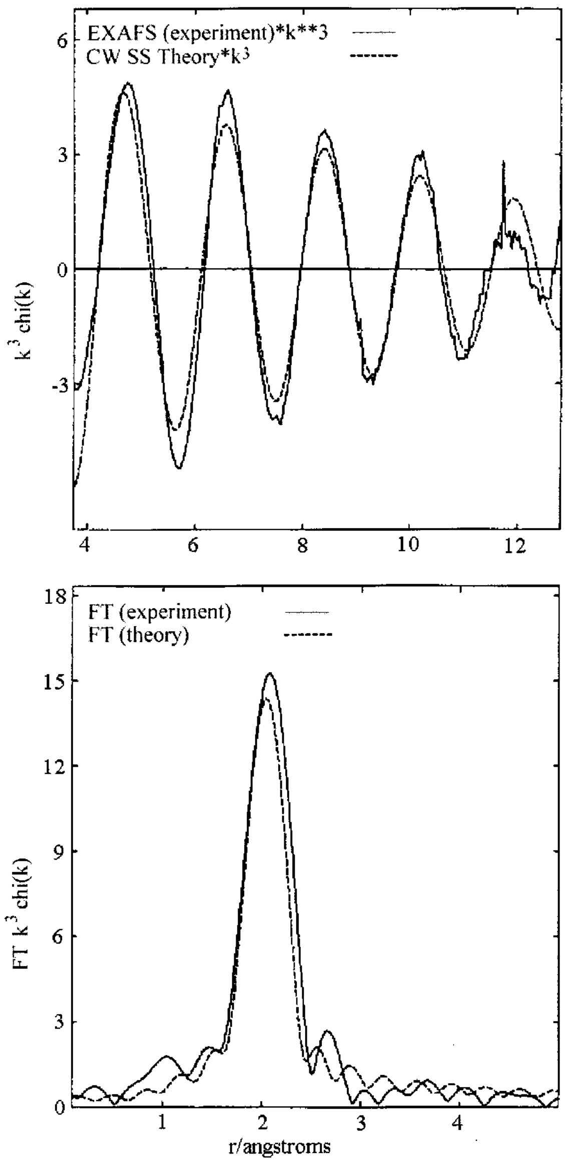

Figure 6. Fe K-edge k^3-weighted EXAFS spectrum and Fourier transform, phase-shift corrected for carbon (—— experimental; ------- curved wave theory, fit B in Table 1), of [Fe{(η-C_5H_4)$_2$SiMe$_2$}] at 298 K

were very large: *R* factor 45.5%, $E°$ −1.8 eV, *r*(Fe−C) 2.023(5) Å, 2 σ^2 0.0236(17) Å^2, *r*(Fe···Si) 2.736(33) Å, 2 σ^2 0.0176(83) Å^2. A better fit to the experimental data was obtained by starting from fit A and refining the coordination number (fit B, Table 1, Figure 6). The final value was 4.3 but the error in this value must be much higher than 20% for the reasons outlined above.

Conclusion

The pore walls of mesoporous siliceous MCM-48 have been successfully derivatized with (1,1′-ferrocenediyl) dimethylsilane. The organometallic complexes react with the MCM-48 surface silanols (particularly of the Q^3 type) to give a $C_5H_4SiMe_2$−O linkage to the silica surface. Despite the fact that MCM-48 and MCM-41 possess very different mesoporous surfaces, this process strongly resembles the process previously reported for the functionalization of the latter by strained ferrocenophanes.

Experimental Section

General: All preparations and manipulations were performed using standard Schlenk techniques under an oxygen-free and water-free argon atmosphere. Pentane was dried by reflux over Na/benzophenone ketyl, distilled under argon, and kept over 4-Å molecular sieves. − Powder X-ray diffraction (XRD) data were collected on a Philips Xpert diffractometer using Cu-K_α radiation filtered by Ni. − Microanalyses were performed at the TU Munich. − Infrared spectra were recorded on a Unican Mattson Mod 7000 FTIR spectrophotometer using KBr pellets and/or solutions. − ^{29}Si- and ^{13}C-NMR spectra were recorded at 79.49 and 100.62 MHz, respectively, on a (9.4 T) Bruker MSL 400P spectrometer. ^{29}Si-MAS NMR spectra were recorded with 40° pulses, spinning rates of 5.0−5.5 kHz, and 60 s recycle delays. ^{29}Si-CP MAS NMR spectra were recorded with 5.5 μs pulses, a spinning rate of 5.0 kHz and 5 s recycle delays. Chemical shifts are quoted in parts per million relative to TMS. ^{13}C-CP MAS NMR spectra were recorded with 4.5 μs pulses, a spinning rate of 8 kHz, and a 4 s recycle delay. Chemical shifts are quoted in ppm relative to TMS. − Nitrogen adsorption isotherms were recorded using a CI electronics MK2-M5 microbalance connected to a vacuum manifold line. The as-made MCM samples (typically around 0.02 g) were dehydrated overnight at 723 K to an ultimate pressure of 10^{-4} mbar, and then cooled to room temperature prior to adsorption. Extra care with the functionalized materials was necessary and so the samples were dehydrated at 423 K to prevent the destruction of the functionalities. Nitrogen isotherms were then recorded at 77 K. Equilibration of each data point was monitored using CI electronics Labweigh software, and the pressure monitored using an Edwards Barocel pressure sensor. Specific surface areas, A_{BET}, were determined from the linear part of the BET equation (P/P_o = 0.05−0.3). − Fe K-edge X-ray absorption spectra were collected at room temperature in transmission mode on station 9.2 [double crystal Si(220) order-sorting monochromator, 50% harmonic rejection] of the Synchrotron Radiation Source at the Daresbury Laboratory, operating at 2 GeV in single bunch mode, with typical currents of 13−19 mA. Solid samples, diluted if necessary with boron nitride, were held between layers of mylar film in 0.5 mm thick aluminium plates. Two spectra were recorded for each sample and summed using the program EXCALIB, available on the Daresbury computer XRSSERV1. The program EXBACK was used to extract the raw EXAFS, $\chi^E(k)$, and curve-fitting analyses, by least-squares refinement of the non-Fourier filtered k^3-weighted EXAFS data, were carried out within EXCURVE (version EXCURV98[13]) using spherical wave methods.[14] Phase shifts were calculated using Von Bart ground state and H. Lundqvis exchange potentials.

[Fe{(η-C_5H_4)$_2$SiMe$_2$}] was prepared by the method reported by Wrighton[15] and purified by sublimation under vacuum.

MCM-41 was synthesized according to the literature employing [($C_{14}H_{29}$)NMe$_3$]Br as a templating agent.[16] After calcination (540°C/6 h) and dehydration (200°C under a vacuum 10^{-4} Torr for 8 h) the material was characterized by XRD, N_2 adsorption and IR spectroscopy.

MCM-41/[Fe{(η-C_5H_4)$_2$SiMe$_2$}] was prepared as described in the literature.[4] Elemental analysis indicated 8.33 mass-% Fe. − IR

(KBr, $\tilde{\nu}$, cm^{-1}): 3574 vs, 3096 m, 2963 m, 1645 s, 1365 m, 1234 vs, 1169 vs, 901m, 816 s, 798 s, 667 m. − (^1H, ^{13}C, ^{29}Si) NMR data are in agreement with ref.[4]

MCM-48 was synthesized according to the literature employing $[(C_{16}H_{33})NMe_3]Cl$ as a templating agent.[17,10b] After calcination (540 °C/6 h) and dehydration (220 °C under a vacuum 10^{-4} Torr for 6 h) the material was characterized by XRD, N_2 adsorption and IR spectroscopy.

Preparation of MCM-48/$[Fe\{(\eta\text{-}C_5H_4)_2SiMe_2\}]$: A suspension of MCM-48 (0.5 g) in pentane (15 mL) was treated with a solution of $[Fe\{C_5H_4)_2SiMe_2\}]$ (0.35 g) in pentane. After 24 h at room temperature, the resulting suspension was filtered off and the remaining orange solid was washed several times with pentane, and dried under an oil-pump vacuum. The pentane washings contained trace amounts of the starting material $[Fe\{(\eta\text{-}C_5H_4)_2SiMe_2\}]$ and ferrocene, identified by solution ^1H-NMR spectroscopy. − Elemental analysis indicated 8.18 mass-% Fe. − IR (KBr, $\tilde{\nu}$ cm^{-1}): 3454 vs, 3103 m, 2960 m, 1637 s, 1423 m, 1234 vs, 1169 vs, 1081 vs, 968 m, 900m, 822 s, 798 s, 667 m, 453 s.

Acknowledgments

We thank PRAXIS XXI and FEDER for partial funding. P. Ferreira (BD) thanks PRAXIS XXI for a grant. I.S.G. wants to thank the CRUP (Acções Integradas Programme) for generous support.

---

[1] J. S. Beck, J. C. Vartuli, W. J. Roth, M. E. Leonowicz, C. T. Kresge, K. D. Schmitt, C. T.-W. Chu, D. H. Olson, E. W. Sheppard, S. B. McCullen, J. B. Higgins, J. L. Schlenker, *J. Am. Chem. Soc.* **1992**, *114*, 10834.

[2] [2a] K. Moller, T. Bein, *Chem. Mater.* **1998**, *10*, 2950. − [2b] T. Maschmeyer, *Curr. Opin. Solid State Mater. Sci.* **1998**, *3*, 71.

[3] V. Alfredsson and M. Anderson, *Chem. Mater.* **1996**, *8*, 1141.

[4] [4a] S. O'Brien, J. Tudor, S. Barlow, M. J. Drewitt, S. J. Heyes, D. O'Hare, *Chem. Commun.* **1997**, 641. − [4b] S. O'Brien, J. M. Keates, S. Barlow, M. J. Drewitt, B. R. Payne, D. O'Hare, *Chem. Mater.* **1998**, *10*, 4088.

[5] I. Manners, *Adv. Organomet. Chem.* **1995**, *37*, 131.

[6] B. Marler, U. Oberhagemann, S. Vortmann, H. Gies, *Microporous Mater.* **1996**, *6*, 375.

[7] X. S. Zhao, G. Q. Lu, A. K. Whittaker, G. J. Millar, H. Y. Zhu, *J. Phys. Chem. B.* **1997**, *101*, 6525.

[8] D. A. Foucher, R. Ziembinski, B.-Z. Tang, P. M. Macdonald, J. Massey, C. R. Jaeger, G. J. Vansco, I. Manners, *Macromolecules* **1993**, *26*, 2878.

[9] K. S. W. Sing, D. H. Everett, R. A. W. Houl, L. Moscou, R. A. Pierotti, J. Rouquerol, T. Siemieniewska, *Pure Appl. Chem.* **1985**, *57*, 603

[10] [10a] A. A. Romero, M. D. Alba, W. Zhou, J. Klinowski, *J. Phys. Chem. B.* **1997**, *101*, 5294. − [10b] J. Xu, Z. Luan, H. He, W. Zhou, L. Kevan, *Chem. Mater.* **1998**, *10*, 3690.

[11] R. Schmidt, M. Stöcker, E. Hansen, D. Akporiaye, O. H. Ellestad, *Microporous Mater.* **1995**, *3*, 443.

[12] W. Finckh, B.-Z. Tang, D. A. Foucher, D. B. Zamble, R. Ziembinski, A. Lough, I. Manners, *Organometallics* **1993**, *12*, 823.

[13] N. Binsted, (**1998**) EXCURV98: CCLRC Daresbury Laboratory computer program.

[14] S. J. Gurman, N. Binsted, I. Ross, *J. Phys. Chem.* **1984**, *17*, 143.

[15] A. B. Fischer, J. B. Kinney, R. H. Staley, M. S. Wrighton, *J. Am. Chem. Soc.* **1979**, *101,* 6501.

[16] C. T. Kresge, M. E. Leonowicz, W. J. Roth, J. C. Vartuli, J. S. Beck, *Nature* **1992**, *359*, 710.

[17] A. Monnier, F. Schüth, Q. Huo, D. Kumar, D. Margolese, R. S. Maxwell, G. D. Stucky, M. Krishnamurty, P. Petroff, A. Firouz, M. Janicke, B. F. Chmelka, *Science* **1993**, *261*, 1299.

Received June 2, 1999
[I99200]